

Modeling of the Vertical Deformations During Exploitation of the Mutnovsky Geothermal Field, Kamchatka

Kiryukhin A.V.¹, Rutqvist J.², Maguskin M.A.¹

¹- Institute of Volcanology and Seismology FEB RAS, Piip-9, Petropavlovsk Kamchatsky 683006 Russia

²- Lawrence Berkeley National Laboratory, 1 Cyclotron Rd, Berkeley, CA 94720, USA

AVKiryukhin2@mail.ru and JRutqvist@lbl.gov

Keywords: Mutnovsky, Subsidence, Thermal-Hydrodynamic-Mechanical, Modeling, Exploitation.

ABSTRACT

Vertical deformation ground leveling was conducted annually in Mutnovsky during 2004-2013 using a network of well markers. Three types of deformation areas with different transient vertical deformation regimes were identified on the basis of these measurements. The first type of deformation area is located in the central part of the Dachny site, where some positive (upward) vertical deformation (2 – 5 mm/year) was observed. The second type of deformation area is located in North reinjection site, where there was no significant vertical deformation observed during 2003-2006, whereas some positive (upward) vertical deformations (6 – 7 mm/year) took place during 2006 – 2008 followed by negative (downward) vertical deformations (5 – 8 mm/year) during 2009-2010. Finally, the third type of vertical deformations is located on Verkhne-Mutnovsky site, where significant subsidence has been taking since 2008 at a rate of 6 – 18 mm/year. Coupled fluid flow and geomechanical simulations with the TOUGH-FLAC simulator were performed using a previously developed TOUGH2 model (Kiryukhin, 2013). THM modeling reasonably explains relative vertical movements during exploitation of the Mutnovsky geothermal field, if considering division of the field by Main Fault into two compartments with different properties for the foot wall block and hanging wall block of the Main Fault.

1. INTRODUCTION

The experience gained at the Mutnovsky geothermal field, Kamchatka, may be useful for development of other large geothermal fields in the Kamchatka-Kurile region, and also for understanding the relationship between volcanic, hydrothermal and seismic activity at similar sites worldwide. Large-scale exploitation at the Mutnovsky geothermal field started in 2000, with fluid extraction of up to 500 kg/s (700 MW), which is comparable to the magma energy rates of two adjacent active volcanoes (Mutnovsky and Gorely). Increased hydrothermal explosion activity of the Mutnovsky volcano appears to be correlated with the exploitation of the geothermal resource. After 40 years of silence, hydrothermal explosions and ash blowouts occurred in the Mutnovsky crater on March 2000, April 2007 (Gavrilenko, 2008), May 2012, and July 2013. Volatile flux emissions from the Gorely volcano started in 2010 with the mass rate estimated to ~130 kg/s (H_2O ~93%, NCG~7% (Aiuppa et al, 2012)), and the crater lakes at both the Mutnovsky and Gorely volcanoes were drained in 2004 and 2012, respectively. Seismic activity also increased within the geothermal field, including 40 earthquakes recorded from February 2009 to December 2013, with K_s ($M=0.5 \cdot K_s - 0.75$) ranging from 4.0 to 7.1, at 2 to 6 km depth.

The Mutnovsky geothermal field is located in the North-Mutnovsky volcano-tectonic (NMVT) zone, which was created by radial fracturing originating from the magmatic systems of the Mutnovsky and Gorely volcanoes as well as local magmatic intrusions. The NMVT zone is clearly delineated by hot springs and fumaroles, and the occurrence of upper Pleistocene rhyolite domes. It includes three segments of different strike: S-NNE, S-NE and EW (see Map in Fig.1, Kiryukhin et al, 2013).

The S-NNE segment also includes the main production fault zone, which supplies a significant fraction of steam to the 50 MWe Mutnovsky power station (Mutnovsky PP) (Kiryukhin, 2005). Geological cross sections along S-NNE segment of the NMVT zone is shown in Fig.1, which demonstrates the following aspects of the geothermal field and adjacent thermal and volcanic features: 1. Production occurs from the recent intrusion contact zone that is traced by the 200-300 °C isotherm range; 2. Production reservoirs are hydraulically connected to the Mutnovsky volcano (recharge area) and adjacent fumaroles and chloride hot springs (4,5,7,9,15,18) (discharge area) through the NMVT zone; 3. Active magma emplacement zone at elevations -4 – -7 km is defined by local earthquakes swarms, where the most plausible conditions for partial melting took place (Simon et al., 2014).

In this paper we present a preliminary coupled THM analysis of ground deformations during exploitation of the Mutnovsky geothermal field. We apply the TOUGH-FLAC simulator (Rutqvist, 2011) that has been previously applied to both generic and site specific studies involving injection, geomechanics, and ground surface deformations (Rutqvist and Tsang 2002; Todesco et al., 2006; Cappa et al., 2009; Rutqvist et al. 2010; Rutqvist et al., 2014). In this first preliminary THM study of the exploitation at the Mutnovsky Geothermal Field, we do not attempt to make an exact inversion of the ground deformation, but we rather focus on a simplified geological representation, yet involving all the key geological features and processes. In particular we investigate whether the observed surface deformation can be explained by pressure- and temperature-induce deformations in the hydrothermal system. We perform a parameter study to investigate how hydrothermal input parameters such as injection rates affect the surface deformations at different areas of the field.

2. GROUND LEVELLING

Vertical deformation ground leveling has been conducted almost annually (in September each year) from 2004 to 2013 on the basis of a network of well markers. A Carl Zeiss, Ni 005A leveling instrument was used and measurement accuracy 1.0 mm/km was achieved. One deep marker located at the western part of the Mutnovsky geothermal field was used as a reference marker

(Reference Point, Fig. 2). Three types of deformation areas with different transient vertical referenced deformation regime were identified on the basis of these measurements (Fig. 2).

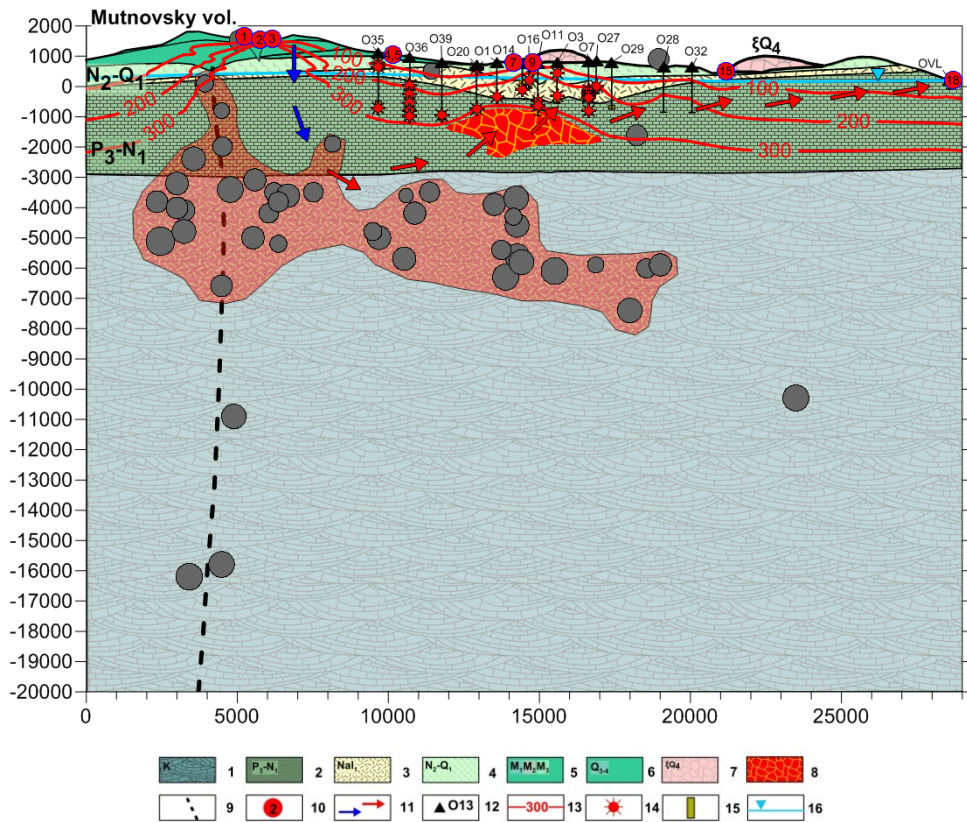


Figure 1: Geological cross sections of the NMVT zone along the S-NNE segment: 1-Basement; 2- Miocene sandstones and tertiary volcano-sedimentary deposits; 3 – Miocene dacite and rhyolite tuffs and lavas; 4 – Pliocene-Quaternary basalts and andesites tuffs and lavas; 5 – Mutnovsky-1, 2 and 3 volcanic cones, respectively; 6 – upper Pleistocene and Holocene andesites and basalts, 7 - rhyolite extrusions; 8 – heat sources (recent magma intrusions); 9 – active feed channel of Mutnovsky volcano; 10 - thermal manifestations (referenced in text); 11 – fluid flows (cold - blue, thermal – red filled); 12 – wells with corresponding numbers; 13 – isotherms, $^{\circ}\text{C}$; 14 – production zones; 15 – wells slotted lines; 16 – water level. Active magma emplacement zone is defined by local earthquakes swarms, which are shown by gray circles, scaled in proportion to magnitude.

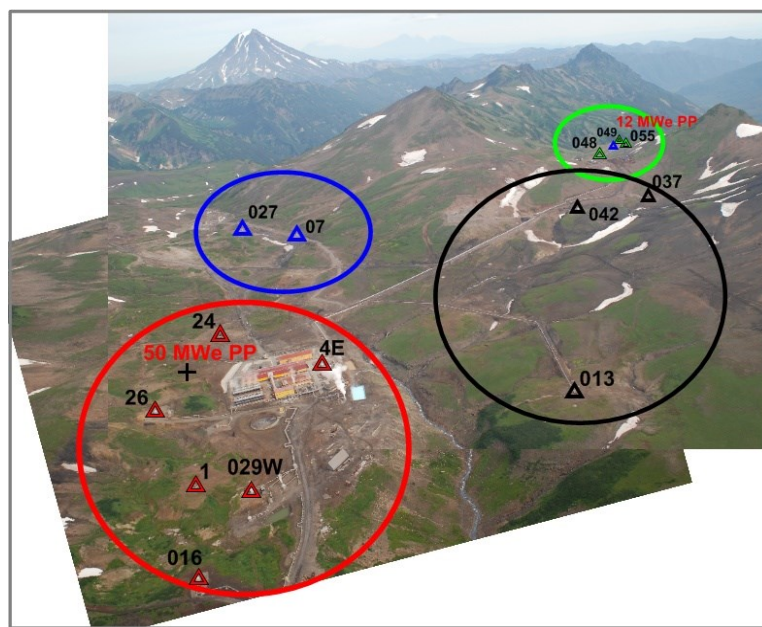


Figure 2: Air photo view of Mutnovsky geothermal field, including production wells of the Central Site (red triangles), East Dachny Site (black triangles), Verkhne-Mutnovsky Site (Green triangles) and reinjection wells (blue triangles). Black cross between wells 26 and 24 is a Reference Point for ground leveling.

The first type of deformation area is located around and south from Mutnovsky PP (west part of the Dachny site). At this location some positive (upward) vertical deformations were observed: 2-4 mm/year from 2004 to 2005, and 3-5 mm/year from 2005 to 2006, after which no significant vertical deformations were observed (Figs. 2 and 3, wells 029W, 26, 4E). An initial hypothesis is that this surface rise may be caused by boiling propagation into the deep high temperature parts of geothermal reservoir with subsequent pressure increase in the shallow steam zone under the low permeability caprock. Potential hydrothermal steam-explosion conditions that could result in such an uplift mechanism have been indicated by several lines of observations at this location. Indeed, steam explosions occurred in this area in 1989 (during drilling of well 029) and in 2003 (near well 022). At that time some of the wells (01, 08, 023) in this area had wellhead temperatures up to 240°C at 33.5 bars pressure indicating hydrothermal explosion conditions at depth.

The second type of deformation area is located at the North Reinjection Site (Figs. 2 and 3, well 027). At this site some positive (upward) vertical deformations (6 – 7 mm/year uplift) took place during 2006 to 2008, followed by negative (downward) vertical deformations (5-8 mm/year subsidence) from 2009 to 2010. It maybe hypothesized that these transient vertical deformations indicate that some reinjection was performed in well 027 during 2006 to 2008, whereas no significant reinjection was performed from 2003 to 2006 and from 2009 to 2010.

The third type of vertical deformations is located at the Verkhne-Mutnovsky site (Fig. 2 & 3, wells 049N, 055, 048). At this location significant subsidence has been taking place since 2008 with a rate of 6 – 18 mm/year. Total subsidence at Verkhne-Mutnovsky PP site amounted to 50 mm by 2013 (accuracy of estimates is 2.5 mm). Similar behavior was observed in the east part of the Dachny site (Fig. 2 & 3, wells 042, 013, 037). This subsidence indicates that the most significant reservoir pressure depletion caused by exploitation occurs in the east part of the Mutnovsky geothermal field.

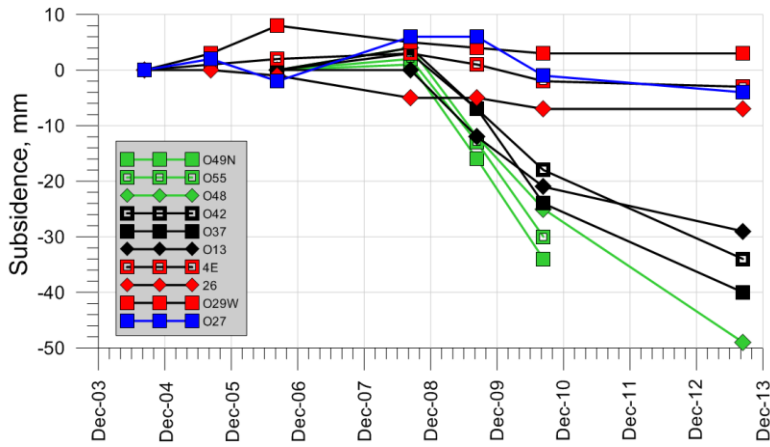


Figure 3: Vertical surface deformation (measured at well marks relative to Referenced Point (see Fig. 2)) data: green – Verkhne-Mutnovsky site wells, black – Dachny site (east part) wells, red – Dachny site (west part) wells, blue – North reinjection site well.

3. THERMAL HYDRODYNAMIC (TH) MODEL (TOUGH2)

In this preliminary analysis a simplified 3D rectangular single porosity TOUGH2 model of 500+ elements (Kiryukhin et al, 2013) was developed and tested against historic exploitation data. This includes exploitation data from 1984 to 2006 (natural state temperatures, pressures, transient production wells enthalpies and reservoir pressures) and additional available data until 2012. The additional data until 2012 includes: (1) transient total steam production for the time period 2007-2008, (2) transient reservoir pressure for 2007-2009, (3) transient chloride in ten production wells for 2002-2006, and (4) non-condensable gas transient change in well 26 for 2000-2010. The final TOUGH2 hydrodynamic (TH) model shown in Fig. 4 adequately models the observed TH responses in the field and this TH model is linked to a geomechanics model and used for the coupled THM analysis that will be presented in the next section.

4. THERMAL HYDRODYNAMIC MECHANICAL (THM) MODEL (TOUGH-FLAC).

The TOUGH-FLAC simulator links the TOUGH family multiphase fluid and heat transport codes with the commercial FLAC3D geomechanics simulator. The earliest developments of TOUGH-FLAC at the Lawrence Berkeley National Laboratory (LBNL) were presented in Rutqvist et al. (2002). TOUGH-FLAC has previously been applied to model crustal deformations caused by deep underground fluid movements and associated pressure and temperature changes as a result of both industrial activities (the In Salah CO₂ Storage Project in Algeria and the Geysers Geothermal Field in California) and natural events (the 1960s Matsushiro Earthquake Swarm in Japan and Flegrean Fields in Italy) (Rutqvist, 2011).

In a TOUGH-FLAC simulation the data exchanges between TOUGH and FLAC3D as transmission of the effective stress σ and strain ϵ (computed in FLAC3D) to TOUGH for calculation of updated porosity ϕ and permeability k by means of empirical equations. The updated ϕ and k values are in turn used to estimate changes in the hydraulic and wettability properties of the porous medium (i.e., aqueous- and gas-phase relative permeabilities and capillary pressure).

The flow of data obtained from TOUGH (namely pressure P , temperature T , and phase saturations S_β) to FLAC3D for processing and estimates their impact on the effective stress $\alpha\Delta P_\beta$ (α being Biot's effective stress parameter), as well as on thermal strain $\epsilon_T =$

$\alpha_T \Delta T$ (α_T being the thermal expansion coefficient). Additionally, changes in P, T, and S_β may also result in changes in other mechanical properties: bulk modulus K, shear modulus G, cohesion C, and coefficient of internal friction μ .

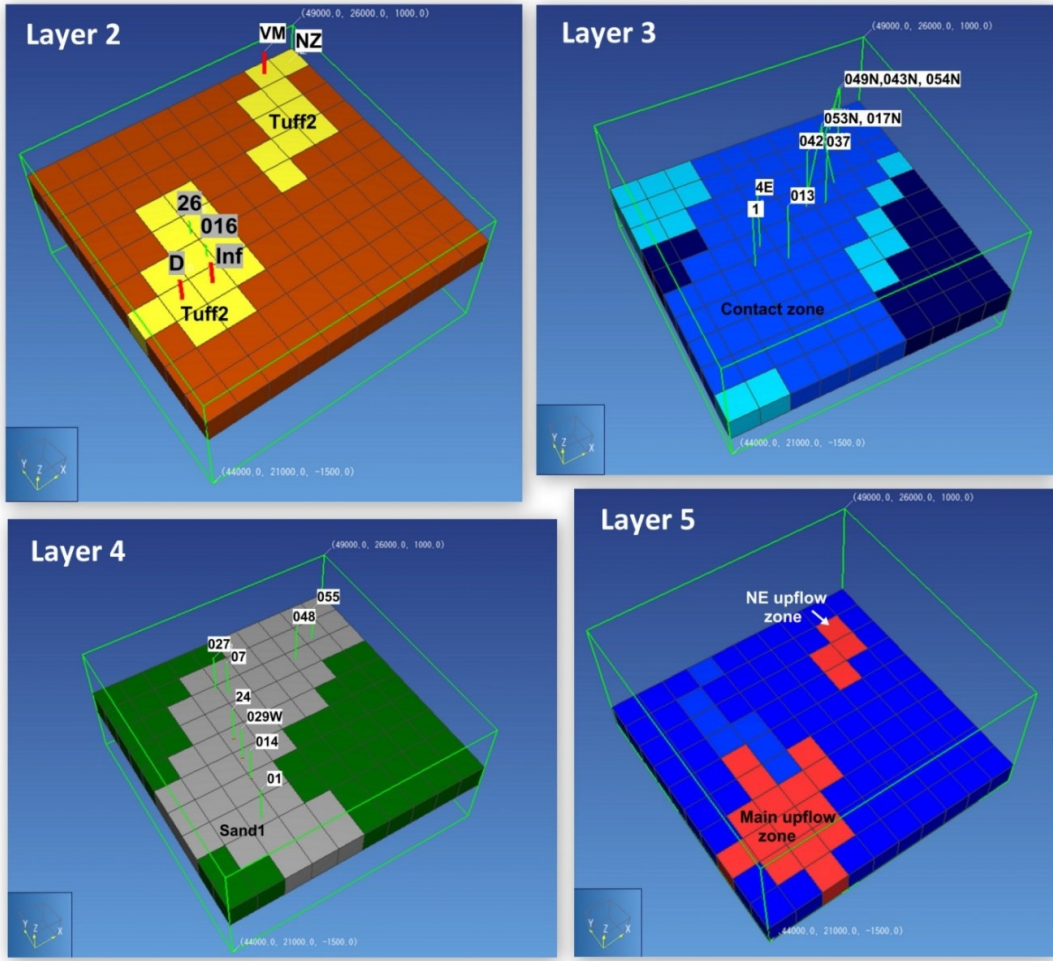


Figure 4: Mutnovsky model layers: Layer 2 (located at +250 masl), includes the permeable reservoir domain “Tuff2”, representing rhyolite tuffs and discharge elements of the model: D – Dachny fumaroles, VM – Verkhne-Mutnovsky fumaroles, NZ – integrated Nizhne-Zhirovskoy hot springs discharge area; Layer 3 (at -250 masl), includes the permeable reservoir domain “Sand1”, representing volcanogenic-sedimentary units; Layer 4 (at -750 masl) includes the permeable reservoir domain “Cont1”, representing intrusion contact zone; Layer 5 (Base layer, -1250 masl) includes Upflow zones (Main and North-East (NE)). Production wells penetrating corresponding layers are shown by numbers on a grey background.

The coupling of TOUGH and FLAC3D is equivalent to the coupling of a finite volume reservoir simulator to a finite element geomechanical simulator, hence numerical grids for the two codes have the same geometry and element numbering. In this preliminary THM simulation of ground deformations at the Mutnovsky Geothermal Field, we limit our analysis to effects of poro-elastic and thermal-elastic responses in the hydrothermal system. The key input material parameters are the elastic properties (bulk modulus and shear modulus), the thermal expansion coefficient and Biot’s coefficient. We set the bulk modulus K = 3.33 GPa, shear modulus G = 2 GPa, thermal expansion coefficient $\alpha_T = 1 \times 10^{-5} \text{ }^\circ\text{C}^{-1}$, and Biot’s coefficient $\alpha = 1$. This initial parameter set was taken from modeling of subsidence at the Geysers geothermal field in California (Rutqvist et al., 2014).

5. THM-MODELING OF MUTNOVSKY GEOTHERMAL FIELD HISTORY OF EXPLOITATION 1984-2013

First the calibrated TH model SP_EXPLO+50R (Kiryukhin, 2013) was used as input for subsequent THM modeling. TH model SP_EXPLO+50R is a single porosity version of TH model #12NSEX6A3, which was described in (Kiryukhin, 2013), it is assumed in TH model SP_EXPLO+50R that 50% of production rate is reinjected. The mechanical boundary conditions are zero displacement normal to bottom and lateral boundaries, whereas the top boundary is free to move.

Reference Point for ground leveling (Fig.2) is located in a 10 m deep well in an exploitation part of the production field. It is not really known if this location is stable. Thus THM simulations results are presented here in format of relative values to the Referenced Point starting from 2004 (see Fig.2). THM simulation results for this case show (Fig. 5) up-lift conditions in all points, whereas field data shows subsidence everywhere except for red lines (Central site) and blue lines (North reinjection site), that is, trends in numerical modeling THM results are opposite of those of measurements.

The TH model SP_EXPLO+50R was then revised and modified to SP_EXPLO_THM3F to reasonably increase pressure drop in green and black areas (East Dachny and Verkhne-Mutnovsky sites) in comparison to red area (Central site) (Fig. 2). In order to do

this the following model modifications were done (see Figs 6 and 7): (1) Additional hot springs natural discharge was added in the north part of the model (VL&NZ), which was not accounted before; (2) Additional recharge (INF2) was added in the central part of the model, where a waste water pool is located, which was not considered before. The modified TH model SP_EXPLO_THM3F was run and reservoir pressure drop in the green and black areas (East Dachny and Verkhne-Mutnovsky sites) was found to be greater than that in the red area (Central Dachny Site).

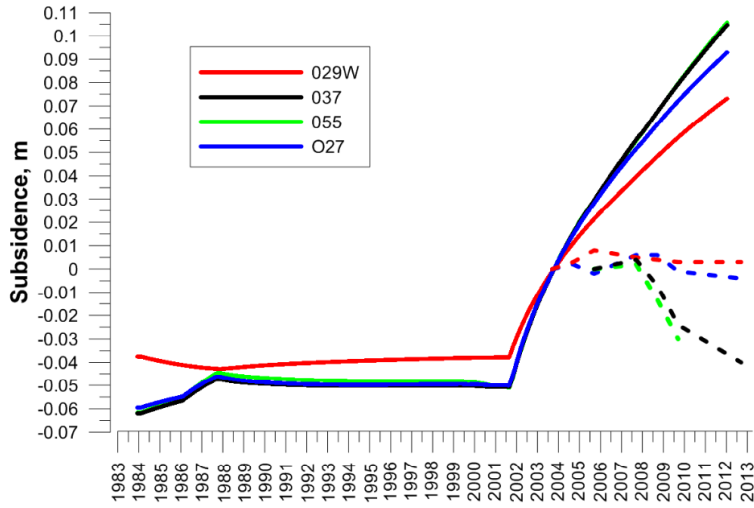


Figure 5: Solid lines are subsidence in THM TOUGH-FLAC simulation, dashed lines are subsidence observations data (Fig. 3). Graphs show subsidence relative to Referenced Point. Lines color corresponds to wells and areas shown in Fig. 2.

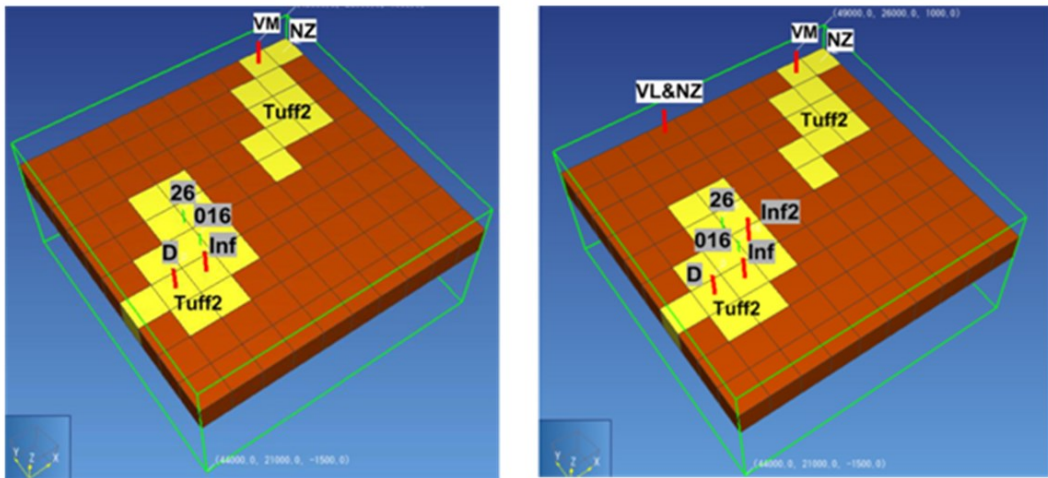


Figure 6: Mutnovsky model SP_EXPLO+50R modification to SP_EXPLO_THM3F (compare left to right figures).



Figure 7: INF2 – corresponds to Power Plant waste water pool, where infiltration of waste water in reservoir may took place, INF corresponds to artificial lake, where cold water infiltration took place.

TOUGH-FLAC simulation SP_JR_3 still shows (Fig. 8) up-lift conditions in all areas, whereas field data shows significant subsidence in green area (Verkhne-Mutnovsky Site) and black area (Eastern Dachny Site).

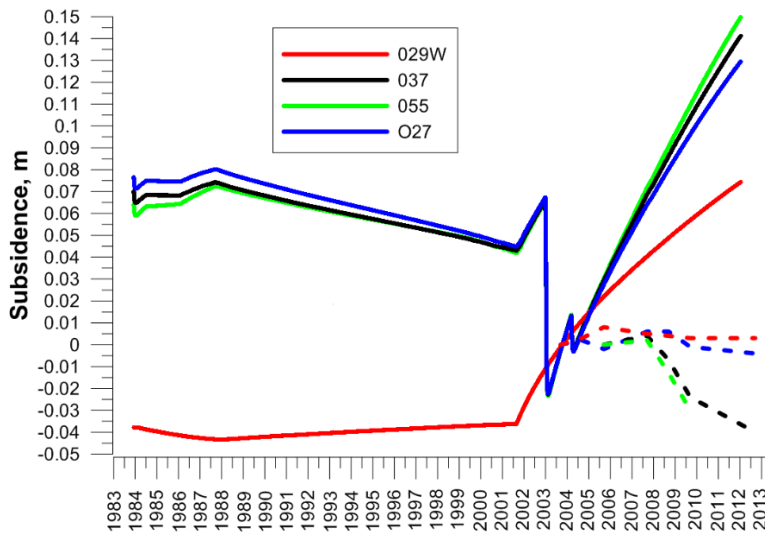


Figure 8: Solid lines are subsidence in TOUGH-FLAC simulation SP_JR_3, dashed lines are subsidence observations data (Fig. 3). Graph show subsidence relative to Referenced Point. Lines color corresponds to wells and areas shown in Fig. 2.

6. DISCUSSION

6.1 General Estimates and Thoughts

In general there is a subsidence in the entire model of about 0.05 m and this is basically caused by small but important pressure and temperature decline in the lowest two layers of the model. For example, the pressure in the two lowest layers decreases about $1.5e5$ Pa. A rough calculation using a Young's modulus of about 5 GPa, and a 1 km thickness (the two layers are totally 1 km thick), leads to a subsidence of $1.5e5$ Pa \times 1000 m / $5e9$ Pa = 0.03 m. This maybe a slight overestimation, but explains the general subsidence. Another additional contribution might be from a general cooling in the lowest two layers. Although simulation results in only 1 degree cooling, such small cooling could still cause some noticeable subsidence: $1 \times 1e-5 \times 1000 = 0.01$ m.

In the modeling there is no significant effect of re-injection at the blue area because the re-injection takes place below 1 km into 1 grid block and this grid block contract and extends locally without much effect up on the ground surface. In the red area, injected water into a grid block at the top surface in a low permeability rock (INF2) causes a pressure change and temperature change, which has very strong effect on surface displacement because the injected element is in direct contact with the top surface.

To obtain a better agreement a possibility would be to model a system where the rock is quite stable around the red, blue and reference point area and at the same time having a larger subsidence at green and black area (Fig. 2). This is the main deformation pattern; a subsidence at green/black and almost stable at red/blue/purple. The small changes up and down at the red/blue area may be induced by small variation in injection there.

The increased subsidence on one side of the field may be explained in terms of a fault, dividing the reservoir into two flow compartments. A slight difference in the pressure decline on one side of the fault could cause the observed differential subsidence. This would be the case if the fault would have low cross-flow permeability and intersect the reservoirs, i.e. dividing the reservoir into two flow compartments. The increased subsidence in green/black compared to red/blue started in 2009 may be related to substantial increase in production in green and black area (on that side of the fault), or (and) the reactivation of the fault as a result of magmatic/tectonic load.

6.2 Magmatic System Activity beneath Mutnovsky Geothermal Field

Local earthquake activity indicates that a large magma emplacement zone (magma chamber) was developed at 5-7 km depth below the Mutnovsky geothermal field (see Introduction and Fig. 1 above). This magma chamber may act as an additional source of deformations of the geothermal reservoir, which was not considered in the current THM model. Possible example of such phenomena was observed, when reservoir pressure rose by 2.4 bars during time period of 14-19 December 2012 in Rodnikovy well (Fig. 9, well location shown in Fig. 1 as OVL well is located 13 km north to Dachny Site) followed by five local earthquakes $Ks=4.0-5.3$ ($M=0.5-Ks-0.75$) next month (data from KF GS RAS) that occurred at elevations of -5 – -6 km below of the Mutnovsky geothermal field (Fig. 10). This seems like a natural “leak-off test” or hydro fracturing event in the roof of the magma chamber beneath the geothermal field. The trace of the fracture plane calculated from those earthquake coordinates is shown on Fig. 10 at elevation -5.8 km. The fracture plane parameters were estimated from eight MEQs swarm coordinates associated with pressure excursions are: dip angle 33°, dip azimuth 138°, horizontal length ~5 km.

6.3 Main Fault

The Main Fault production zone occurs within North-Mutnovsky volcano-tectonic zone (Kiryukhin, 2005). Main fault production zone strikes north-north-east (Fig. 10) with east-east-south dip 60°, and average vertical thickness 240 m. The Main fault production

zone at the Dachny site is penetrated by wells 045, 01, 014, 016, 1, 029W, 26, 24, 4E (Fig.2). The strike of Main fault production zone is sub-parallel to the system of the active faults and recent dykes, some of which are found inside of the Main fault. Roof of the Main fault production zone is identified by circulation losses during drilling. Approximation plane of the Main production zone is defined by the following equation: $Z = -1.691076246561*X + 0.48880109651512*Y + 65583.1$ obtained on the basis of circulation loss and production feed zones coordinates. The approximated plane of the Main production zone intersects the active magma feeding chamber of Mutnovsky volcano at elevations of +250 - +1250 masl and at a distance of 8 km from the production site. Four additional wells (A1-A4) drilled (in 2001-2002 years) and equipped with slotted liners in the foot block of the Main fault production zone have demonstrated zero or low productivity.

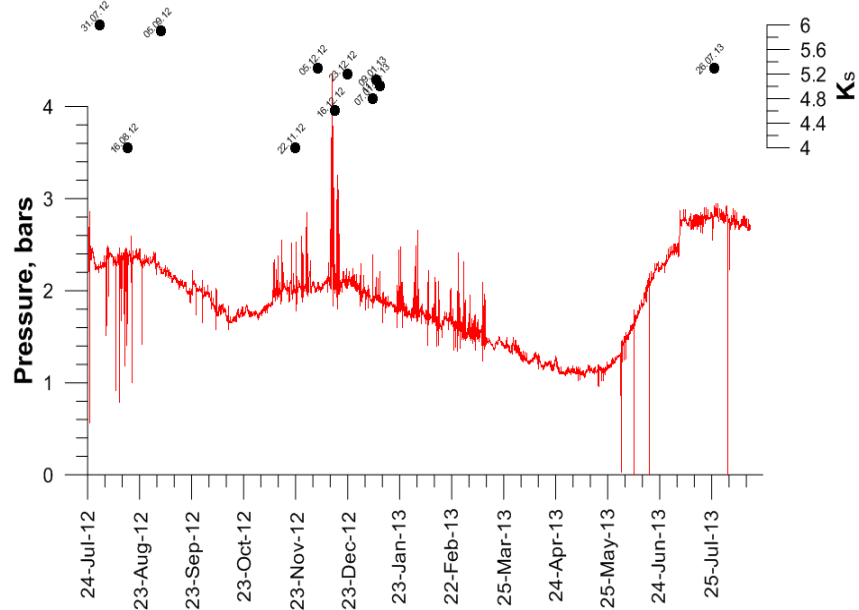


Figure 9: Wellhead pressure in Rodnikovy well vs local earthquakes activity in Mutnovsky geothermal field area (EQ data from KF GS RAS).

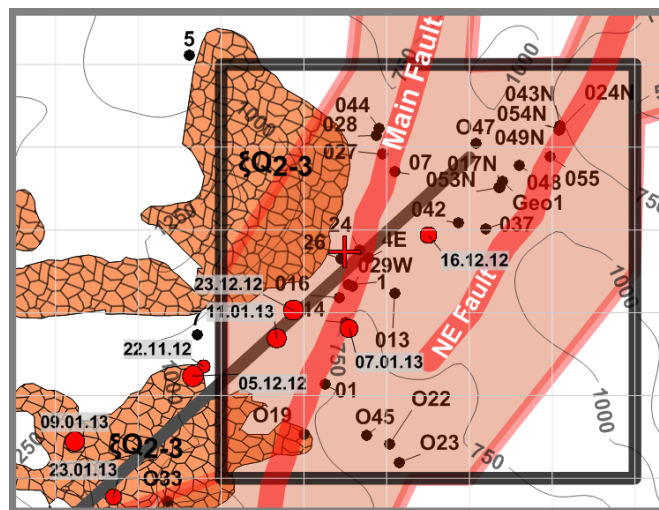


Figure 10: Schematic map of the Mutnovsky geothermal field shows: TH/THM models area (rectangle); wells positions (black circles with numbers); local earthquakes occurred in November 2012 – January 2013 (scaled red circles with dates) positions; thick black line is the trace of the fracture plane calculated from those earthquakes coordinates at elevation -5.8 km; $\zeta Q_{2,3}$ - rhyolite extrusions; North-Mutnovsky volcano tectonic zone – highlighted area, red thick lines – Main Fault Production Zone and North-East Production Zone, correspondingly. Red crest between wells 26 and 24 is a Reference Point for ground leveling.

In the foot block of the Main Fault corresponding rock units are located about 100-150 m above corresponding units in the hanging block, showing that the Main fault is a normal fault. Note that extensional graben-type conditions are assumed for North Mutnovsky Volcano Tectonic Zone (NMVT) as a whole. The Main fault also acts as a semi-permeable fault: the foot wall is impermeable (possibly due to temperature inversions and sealing by secondary hydrothermal minerals), while hanging wall is open to flows into the NE direction

Based on this conceptual model, the numerical model was divided by the Main fault into two parts with different vertical deformations rates caused either by exploitation load, rock properties, and/or by magmatic/tectonic system activity beneath the field (Fig. 11). Red/blue wells are anchored in a foot block of the Main fault, while green/black wells are sliding down in a hanging block.

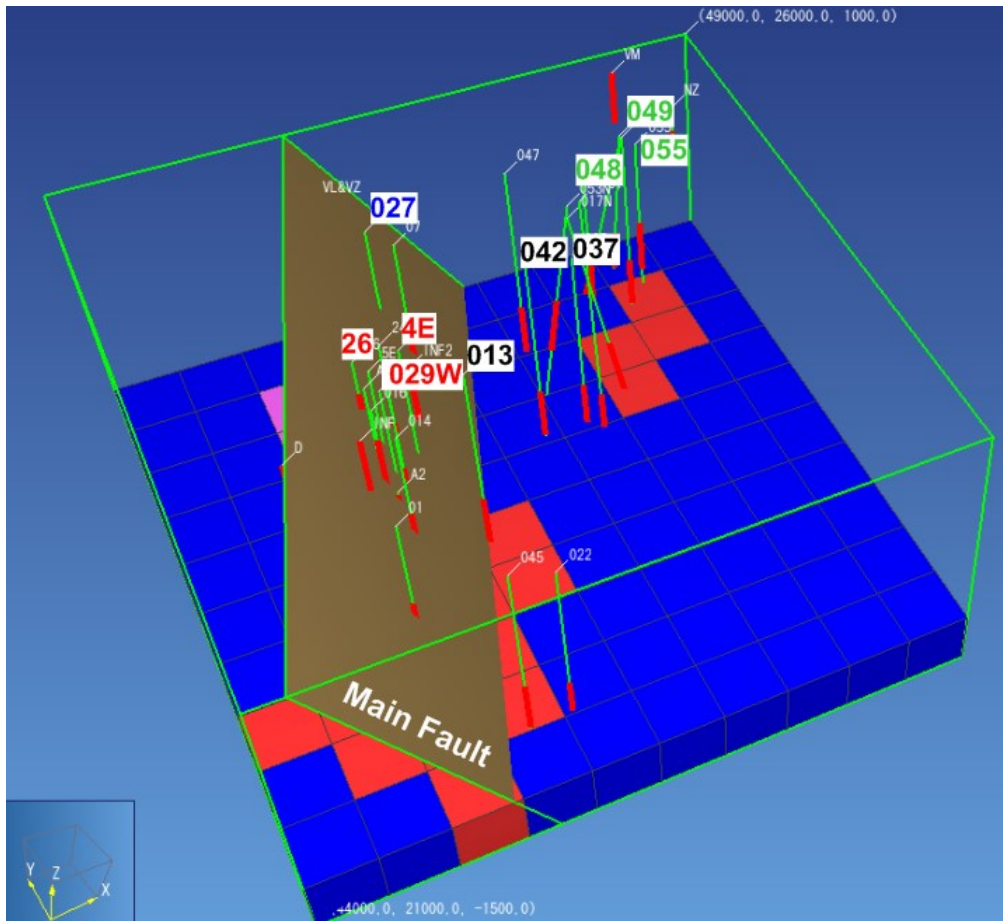


Figure 11: A base layer of Mutnovsky TH model with added internal boundary represented Main Production Fault Zone (Kiryukhin, 2005).

7. THM-MODELING CONSIDERING FAULT DIVIDED RESERVOIR COMPARTMENTS

7.1 Assigning stiffer properties to non-productive foot block

Since Main Fault was found to be a natural semi-permeable boundary which separated Mutnovsky geothermal field on two compartments: productive hanging block and non-productive foot block, it is reasonable to modify a model accordingly to geometry shown in Fig. 11. To realize this, stiffer mechanical properties were assigned in THM model for all elements of the foot block of Main Fault, while the stiffness of elements in the hanging block remains low as before. The calibrated TH model **SP_EXPLO2** (Kiryukhin, 2013) was used as input for subsequent THM modeling. TH model **SP_EXPLO2** is a single porosity version of TH model #12NSEX6A3, which was described in (Kiryukhin, 2013). It is assumed in TH model **SP_EXPLO2** that 50% reinjection was performed, no infiltration through artificial lake (INF1) occurred and infiltration from waste pond INF2 (see Fig. 7) into geothermal reservoir took place with the rate of 200 kg/s.

The TOUGH-FLAC simulation in terms of relative subsidence referenced to 2004 year (start of subsidence observations) significantly improves the match in all observational areas except of red area (Central Site), where THM model is not show 6 mm uplift observed in 2004-2006 years (Fig. 12). Nevertheless, as was shown above, this effect may be accounted in the model by a carefully assigned recharge in the central part of the model, where waste water pool is located (Fig. 7). While improved match to the field data was achieved by simply assigning different mechanical properties on one side of the fault, a much more detailed geologic cross-section may provide further clues on what is the real cause of the differential subsidence. It might be related to different deformability or could be related to differences in hydraulic properties giving rise to difference in pressure depletion and associated compaction. Moreover, the use of satellite based ground surface deformation could provide a much better aerial view of the surface deformation pattern, including delineation of the Main producing fault, and the spatial distribution of the flow compartment on each side of the fault.

7.2 Assigning low permeability to non-productive foot block

Another possibility is to assign low permeability to all model elements in the non-productive foot wall block as shown in Fig. 11. To realize this, TH-model **SP_EXPLO2** was modified accordingly: all elements in foot wall block were assigned with permeability from $1E-18$ m^2 (top three layers of the model) to $3E-16$ m^2 (bottom two layers of the model) (model scenario

SP_EXPLO_THM3F+F2). Surprisingly high relative uplift (+0.17 m) of all sites outside of the waste pool area was observed in a TOUGH-FLAC model due to thermal cooling effect (thermal shrinking of the central part of the geothermal field as a result of injection of 200 kg/s of the waste separated water in the open pool, Fig. 7, INF2). Such high sensitivity of the model to waste water injection rate in the open pool is pointed out to thoroughly study those parameter influence in a range of a possible variation. This sensitivity study is on going.

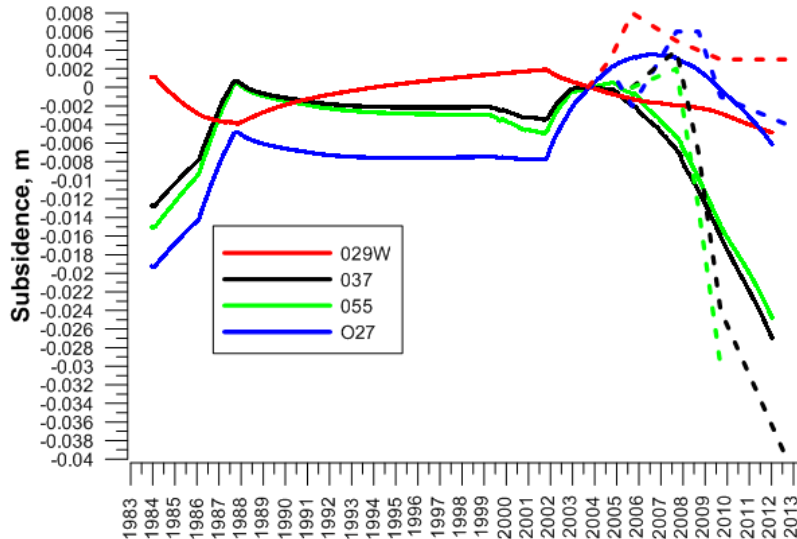


Figure 12: Solid lines are subsidence in TOUGH-FLAC simulation SP_EXPLO2, dashed lines are subsidence observations data (Fig. 3). This graphs show subsidence relative to Referenced Point and 2004 year. Lines color corresponds to wells and areas shown in Fig. 2.

CONCLUSIONS

1. Vertical deformation ground leveling, conducted annually in Mutnovsky during 2004-2013, revealed three types of areas with different transient vertical deformation regimes: Central part of Dachny site was characterized by significant positive vertical deformations (2-5 mm/year); North reinjection site, where some positive vertical deformations occurred (6 – 7 mm/year) during 2006 – 2008 followed by subsidence (5-8 mm/year) during 2009-2010; East Dachny and Verkhne-Mutnovsky site, where significant subsidence has been taking since 2008 at a rate of 6 – 18 mm/year.
2. A thermal-hydrodynamic-mechanical (THM) TOUGH-FLAC modeling was used to attempt to explain observed subsidence during exploitation of the Mutnovsky geothermal field 1984-2010. For these purposes an input TH model developed in Kiryukhin (2013) was used.
3. THM modeling reasonably explains relative vertical movements during exploitation of the Mutnovsky geothermal field, if considering division of the field by the Main Fault into two compartments with larger reservoir compaction in the hanging wall block, or low permeability in foot wall block.

ACKNOWLEDGMENTS

Authors are appreciative to Y.F. Manukhin and The Agency of Natural Resources of Kamchatka for providing input data for Mutnovsky modeling. This work was supported by RFBR under the project 12-05-00125 and FEB RAS under the projects 12-III-A-08-170, 12-I-P27-04.

REFERENCES

Cappa, F., Rutqvist, J., Yamamoto, K. Modeling crustal deformation and rupture processes related to upwelling of deep CO₂ rich fluids during the 1965-1967 Matsushiro Earthquake Swarm in Japan. *Journal of Geophysical Research*, 114, B10304, (2009)/

Kiryukhin, A.V., Modeling Studies: the Dachny Geothermal Reservoir, Kamchatka, Russia. *Geothermics*, V. 25, # 1, (1996) p. 63-90.

Kiryukhin, A.V., Modeling of the Dachny Site Mutnovsky Geothermal Field (Kamchatka, Russia) in Connection with the Problem of Steam Supply for 50 MWe Power Plant // Proceedings World Geothermal Congress 2005 Antalya, Turkey, 24-29 April 2005, 12 p.

Kiryukhin, A.V., Maguskin, M.A., Miroshnik, O.O., Delemen, I.F.: Modeling and Observations of the Enthalpy, Pressure, Chloride, CO₂ and Vertical Deformation Transient Change in the Mutnovsky Geothermal Field (Kamchatka, Russia), *Proceedings*, 38-th Workshop on Geothermal Reservoir Engineering, Stanford University, Stanford, CA (2013).

Kiryukhin, A.V., Rutqvist J., Maguskin M.A.: Thermal-Hydrodynamic-Mechanical Modeling of Subsidence During Exploitation of the Mutnovsky Geothermal Field, Kamchatka, *Proceedings*, 39-th Workshop on Geothermal Reservoir Engineering, Stanford University, Stanford, CA (2013).

Pruess, K., Oldenburg, C. and Moridis, G. TOUGH2 User's Guide, Version 2.0. Report LBNL- 43134, Berkeley, California, (1999).

Rutqvist, J., Wu, Y.-S., Tsang, C.-F., Bodvarsson, G. A modeling approach for analysis of coupled multiphase fluid flow, heat transfer, and deformation in fractured porous rock. *International Journal of Rock Mechanics & Mining Sciences* **39** (2002) 429–442.

Rutqvist, J., Vasco, D., Myer, L. Coupled reservoir-geomechanical analysis of CO₂ injection and ground deformations at In Salah, Algeria. *Int. J. Greenhouse Gas Control*, 4, 225–230 (2010).

Rutqvist, J., Dobson, P.F., Garcia, J., Hartline, C., Jeanne, P., Oldenburg, C.M., Vasco, D.W., Walters, M. The Northwest Geysers EGS Demonstration Project, California: Pre-stimulation Modeling and Interpretation of the Stimulation. *Mathematical Geology*, (published online 17 October 2013). DOI 10.1007/s11004-013-9493-y (2014).

Rutqvist, J. Status of the TOUGH-FLAC simulator and recent applications related to coupled fluid flow and crustal deformations // *Computers & Geosciences* **37**, (2011), 739–750.

Simon, A., Yogodzinski, G.M., Robertson, K., Smith, E., Selyangin, O., Kiryukhin, A., Mulcahy, S. R., Walker, J. D. Evolution and Genesis of Volcanic Rocks 1 from Mutnovsky Volcano, Kamchatka *Journal of Volcanology & Geothermal Research* (2013, submitted), 74 p.

Todesco, M., Rutqvist, J., Chiodini, G., Pruess, K., Oldenburg, C.M. Modeling of recent volcanic episodes at Phleorean Fields (Italy): geochemical variations and ground deformation. *Geothermics* 33, 531-547 (2004).